Probing the π-π^* transitions in conjugated compounds with an infrared femtosecond laser

Xi Liu,[1] Pengcheng Li,[2] Xiaosong Zhu,[1,*] Pengfei Lan,[1] Qingbin Zhang,[1] and Peixiang Lu[1,3,†]

[1]*School of Physics and Wuhan National Laboratory for Optoelectronics, Huazhong University of Science and Technology, Wuhan 430074, China*

[2]*College of Physics and Electronic Engineering, Northwest Normal University, Lanzhou 730070, China*

[3]*Laboratory of Optical Information Technology, Wuhan Institute of Technology, Wuhan 430205, China*

(Received 27 December 2016; revised manuscript received 24 February 2017; published 22 March 2017)

We show that the processes of π-π^* transitions imprint themselves on the high-harmonic spectra when conjugated molecules interact with intense femtosecond laser pulses. It is found that a noninteger order peak appears in the harmonic spectrum with the photon energy equaling the excitation energy of the π-π^* excitation. Further studies prove that this radiation is caused by the π-π^* transition. The transition signals are prominent and can be easily measured as the corresponding radiation intensities are comparable to those of integer order harmonics. Our results pave the way for the study of excited-state electron-ion dynamics using high-harmonic spectroscopy. In comparison to the traditional absorption spectroscopy method relying on the synchrotron radiation source, the present approach is easily accessible for the use of a tabletop laser-based source. Furthermore, our study also provides a potential tool to probe the π-π^* transition processes in femtosecond resolution.

DOI: 10.1103/PhysRevA.95.033421

I. INTRODUCTION

In recent decades, it has been widely recognized that the π-π^* transition [1] plays an important role in many fields of chemistry, biology, and materials science. For example, in the chemical field, plenty of photoreactions, such as double bond isomerizations [2] and electrocyclic reactions [3], have been interpreted by the π-π^* transitions between molecular frontier π and π^* orbitals [4]. Based on the π-π^* transition, acetylacetone was used to produce the OH radical induced by ultraviolet (UV) irradiation [5]. In the biological field, the process of the π-π^* transition is essential for understanding the luminous mechanism of biological chromophores [6], such as the green fluorescent protein [7]. Also, the same transition process impacts the optical characteristics of xDNA base assemblies [8]. In film surfaces of various kinds of nylons, the different delocalization characters of π-π^* transitions and transition dipole couplings are associated with the crystal structure pattern and intermolecular hydrogen bonding [9]. The π-π^* transitions in organic molecules have been widely studied in both theory [10–13] and experiment [14,15].

Characteristic and efficient π-π^* transitions take place in conjugated compounds [16]. The conjugated compound is composed of alternating multiple (double or triple) and single bonds. Due to the conjugated structure, electrons in conjugated compounds are delocalized over the π bond system, which leads to the lower energy and greater stability of the molecule. In a conjugated compound, a strong π-π^* transition occurs when an electron is excited from the π-type highest occupied molecular orbital (HOMO) to the π-type lowest unoccupied molecular orbital (LUMO) [17]. Hence, the excitation energy of the π-π^* transition depends on the HOMO-LUMO energy gap, which has a close relation to the extent of the chain composed of alternating multiple and single bonds [18]. Traditionally, the excitation dynamics of conjugated systems are studied by UV absorption spectroscopy [19]. In the optical absorption spectrum, a sharp absorption peak appears at the position where the photon energy equals the π-π^* excitation energy. The corresponding wavelength is called maximum absorption wavelength λ_{max}. For molecules with large HOMO-LUMO energy gaps, the effective measurements of optical absorption require a synchrotron radiation (SR) source [20,21]. However, the SR source is unapproachable since the SR facility is huge, bulky, and expensive. Moreover, the time resolution available from the SR is typically just in the picosecond scale, which is too low to probe electronic dynamics [22]. Therefore, an easily accessible method in the natural time scale of electronic dynamics to study the π-π^* excitation processes becomes an urgent demand.

With the development of intense ultrashort laser technology, high-harmonic spectroscopy (HHS) opens up a new frontier to study the laser-matter interactions [23–25]. High harmonics are a series of integer order radiations that are generated when intense femtosecond laser pulses interact with atoms or molecules [26]. As an ultrafast nonlinear process, high-harmonic generation (HHG) makes it possible to get insight into electronic structures and probe electronic dynamics in a femtosecond and even subfemtosecond time scale. This feature of HHG helps people better understand the microscopic world. For example, the electronic orbitals of molecules can be imaged with subfemtosecond resolution using amplitudes and phases of high harmonics [27–30]. In addition, the chiral HHG method paves a way to probe the molecular chirality on a subfemtosecond time scale [31–33]. Owing to the interferences of different channels, the attosecond multielectron dynamics of molecules in an intense laser field are revealed by high-harmonic interferometry [34]. Based on HHS, the attosecond charge migration process can be also resolved spatially and temporally [35]. Also, HHG provides an effective tool to map the process of chemical reactions [36]. The ability to follow the evolution of electronic wave packets on their natural time scale has been a major concern of attosecond science in the past two decades [37,38].

*zhuxiaosong@hust.edu.cn

†lupeixiang@mail.hust.edu.cn

Recently, HHG involving excited states below and near the ionization threshold has attracted much attention. For example, Beaulieu *et al.* [39] experimentally demonstrate that the populations of excited states influence the HHG by two pathways. The first one is called e-HHG [40,41], which occurs when the electrons are ionized from excited states and recombine to the ground state. The other one is the free induction decay (FID) process [42,43]. In this process, first an electron is captured into an excited state with long lifetime. Then it will give rise to a narrow-band radiation at the field-free resonance energy via subsequently spontaneous emission.

Herein, we investigate the high-harmonic generation of conjugated molecules benzene and *trans*-1,3-butadiene driven by an infrared femtosecond laser using time-dependent density functional theory (TDDFT). It is found that a sharp noninteger order peak locates in the low-energy region of the harmonic spectrum, and the corresponding photon energy is consistent with the π-π^* excitation energy shown in the optical absorption spectrum. The photon energy of the noninteger order peak remains the same when the wavelength of the laser pulse is changed. Our study shows that the noninteger order radiation peak is also caused by the π-π^* transition. Unlike the optical absorption response, this transition is the inverse process of the optical excitation transition, i.e., this transition occurs from the LUMO(s) to HOMO(s). This mechanism is further confirmed by investigating the dependency relationship between the radiation intensity and the elevation angle of the laser field. This work extends the scope of HHS and establishes it as a potential tool for studying excited-state dynamics and photoexcitation processes. Compared with a traditional absorption spectroscopy method using a SR source, the HHS method has the advantages of accessibility and high temporal resolution.

II. THEORETICAL MODEL

In this work, the harmonic spectra and optical absorption spectra of the benzene and *trans*-1,3-butadiene are calculated using the three-dimensional (3D) TDDFT [44]. This methodology is an attractive alternative to study HHG and optical absorption due to its natural inclusion of multielectron dynamics [45–50]. In the TDDFT method, the evolutions of systems are described by a set of auxiliary noninteracting one-particle Kohn-Sham orbitals, which satisfy the time-dependent Kohn-Sham (TDKS) equations (atomic units are used throughout this paper unless otherwise stated)

$$i\frac{\partial}{\partial t}\psi_i(\mathbf{r},t) = \left[-\frac{\nabla^2}{2} + v_s(\mathbf{r},t)\right]\psi_i(\mathbf{r},t)\ (i = 1,2,\ldots,N). \tag{1}$$

In Eq. (1), N different Kohn-Sham orbitals $\psi_i(\mathbf{r},t)$ are propagated in time. The time-dependent electron density $n(\mathbf{r},t)$ is constructed by $n(\mathbf{r},t) = \sum_{i=1}^{N} |\psi_i(\mathbf{r},t)|^2$. The time-dependent Kohn-Sham potential v_s is a functional of this density and is defined as

$$v_s(\mathbf{r},t) = \int \frac{n(\mathbf{r}',t)}{|\mathbf{r}-\mathbf{r}'|}d\mathbf{r}' + v_{\mathrm{xc}}(\mathbf{r},t) + v_{ne}(\mathbf{r}) + v_{\mathrm{ext}}(\mathbf{r},t). \tag{2}$$

$v_{\mathrm{xc}}(\mathbf{r},t)$ is the exchange-correlation potential accounting for all nontrivial many-body effects. Here, we apply the general gradient approximation in the parametrization of Perdew-Burke-Ernzerhof [51]. $v_{ne}(\mathbf{r})$ represents the interaction between valence electrons and the ionic core, and is modeled by norm-conserving Hartwigsen-Goedecker-Hutter pseudopotentials [52]. $v_{\mathrm{ext}}(\mathbf{r},t)$ is the external potential due to external laser fields. The TDKS equations are propagated in time using the approximated enforced time-reversal symmetry [53] scheme. The unphysical reflections are overcome by adding an absorptive boundary on the wave functions at the edge of the grid.

In the HHG response, the interaction term of full Hamiltonian is treated in dipole approximation as $v_{\mathrm{ext}}(\mathbf{r},t) = \mathbf{r}\cdot\mathbf{F}(t)$, where $\mathbf{F}(t)$ is the electric field of the laser pulse. We adopt a trapezoidal envelope with a total duration of eight optical cycles (with two-cycle linear ramps and four-cycle constant center). The harmonic intensity is calculated from the Fourier transform of the dipole acceleration:

$$H(\omega) = \left|\int \ddot{\mathbf{d}}(t)e^{i\omega t}dt\right|^2, \tag{3}$$

where the time-dependent dipole $\mathbf{d}(t)$ is given by

$$\mathbf{d}(t) = \int n(\mathbf{r},t)\mathbf{r}\,d\mathbf{r}. \tag{4}$$

In order to obtain the optical absorption spectrum in a given direction, such as the z direction, we excite all frequencies of the system by adopting a kick electric field $v_{\mathrm{ext}}(\mathbf{r},t) = -\kappa z\delta(t)$ [16,54], which is equivalent to imposing a short-duration small momentum κ on the electrons. The Kohn-Sham orbitals at time δt can be analytically obtained as $\psi_i(\mathbf{r},\delta t) = e^{i\kappa z}\psi_i(\mathbf{r},0)$. After the time-dependent propagation, the absorption intensity can then be obtained from the dipole strength function $S(\omega)$ written as

$$S(\omega) = \frac{2\omega}{\pi}\mathrm{Im}[\alpha(\omega)], \tag{5}$$

where $\alpha(\omega)$ is the dynamical polarizability and is obtained by

$$\alpha(\omega) = \frac{1}{\kappa}\int d(t)e^{i\omega t}dt. \tag{6}$$

In our numerical simulations, all calculations are performed with the OCTOPUS [55] package. We use the spatial spacing of 0.3 a.u. and the time step of 0.02 a.u. The ionization potentials I_p obtained by the ground-state calculation is 9.230 eV for the benzene and 8.822 eV for the *trans*-1,3-butadiene, which are consistent with the experiment values [56] ($I_p = 9.250$ eV for the benzene and $I_p = 9.080$ eV for the *trans*-1,3-butadiene).

III. RESULTS AND DISCUSSIONS

Figure 1(a) shows the calculated optical absorption spectra of the benzene for the x and z directions. Herein, the benzene molecule lies in the x-y plane. The coordinate system is presented at the top of Fig. 1(b). The kick momentum κ is 0.01 a.u., and the time evolution is run for a maximum time $T = 800$ a.u. In Fig. 1(a), it is shown that a narrow peak appears at 6.85 eV in the absorption spectrum for the x direction. This prominent absorption originates from the π-π^* transition, and the position of this peak corresponds to the excitation energy ΔE. Our results are in agreement with

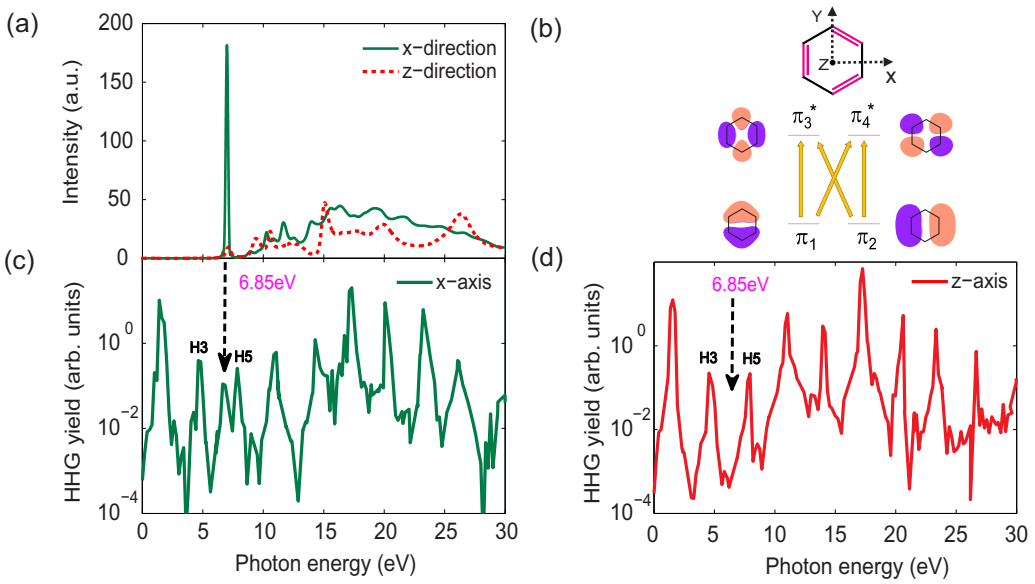

FIG. 1. (a) The optical absorption spectra of the benzene for the x and z directions. (b) The schematic illustration of the π-π^* transition between the HOMOs (π_1 and π_2) and LUMOs (π_3^* and π_4^*) of the benzene in the optical absorption response. The geometrical configuration of the benzene molecule and the coordinate system are presented at the top. (c) and (d) The high-harmonic spectra of the benzene driven by laser pulses polarized in the x axis and z axis, respectively. The wavelength of the laser pulse is 800 nm and the laser intensity is 8×10^{13} W/cm^2.

the experimental observation and the theoretical simulation, where the excitation energy ΔE is around 6.90 eV ($\lambda_{\max} \approx$ 179.7 nm) [12,16,20]. The process of the absorption response is illustrated in Fig. 1(b). As shown in Fig. 1(b), the HOMOs (π_1 and π_2) and LUMOs (π_3^* and π_4^*) of the benzene are doubly degenerate π orbitals. When excited with light, the electron undergoes a transition from HOMOs to LUMOs, accompanied by an absorption of a photon. The transitions between those states are responsible for the strong absorption at 6.85 eV. Table I presents the transition dipole moments $\mathbf{d}_{\pi\text{-}\pi^*}$ between HOMOs and LUMOs. $\mathbf{d}_{\pi\text{-}\pi^*}$ is obtained by $\mathbf{d}_{\pi\text{-}\pi^*} = \langle\psi_\pi|\mathbf{r}|\psi_{\pi^*}\rangle$, where ψ_π and ψ_{π^*} are Kohn-Sham wave functions of the π and π^* orbitals, respectively. According to Table I, one can see that x components of $\mathbf{d}_{\pi_1\text{-}\pi_3^*}$ and $\mathbf{d}_{\pi_2\text{-}\pi_4^*}$ are zeros. Hence, the absorption in the x direction is only attributed to the π_1-π_4^* and π_2-π_3^* transitions. Similarly, the absorption in the y direction is only attributed to the π_1-π_3^* and π_2-π_4^* transitions. The z components of all $\mathbf{d}_{\pi\text{-}\pi^*}$ (includes $\mathbf{d}_{\pi_1\text{-}\pi_3^*}$, $\mathbf{d}_{\pi_1\text{-}\pi_4^*}$, $\mathbf{d}_{\pi_2\text{-}\pi_3^*}$, and $\mathbf{d}_{\pi_2\text{-}\pi_4^*}$) of the benzene shown in Table I are zeros. This indicates that the π-π^* transition in the z direction is forbidden. The optical absorption spectrum of the benzene for the z direction is shown in Fig. 1(a). One can see that no obvious absorption peak appears at ΔE. The result is consistent with the fact that the π-π^* transitions in the z direction are forbidden.

The high-harmonic spectrum of the benzene driven by the laser pulse polarized in the x axis is shown in Fig. 1(c). The wavelength of the laser pulse is 800 nm and the laser intensity is 8×10^{13} W/cm^2. This laser pulse can be easily accessed using a commercial tabletop Ti:sapphire femtosecond laser system in optical laboratories. It is shown that the harmonic spectrum is composed of a series of radiation peaks whose frequencies are odd multiples of the driving laser frequency. These peaks present the typical high harmonics. Besides these integer order harmonics, there is a remarkable noninteger order radiation peak between the third harmonic and the fifth harmonic in Fig. 1(c). The intensity of this radiation peak is comparable to those of integer order harmonics. It is worth noting that, as the black dashed arrow indicates, the photon energy of this radiation peak is equal to the π-π^* excitation energy shown in Fig. 1(a). The coincidence between the photon energy of the noninteger order radiation and the π-π^* excitation energy implies that this radiation may originate from the π-π^* transitions from LUMOs to HOMOs, i.e., the inverse processes of the optical absorption response. When conjugated systems are irradiated by an external intense femtosecond laser pulse,

TABLE I. Transition dipole moments between the HOMOs and LUMOs.

Molecular species	Dipole transition	Transition dipole moment (a.u.)		
		x	y	z
benzene	π_1-π_3^*	0.0000000	1.4437995	0.0000000
	π_1-π_4^*	−1.4436732	0.0000000	0.0000000
	π_2-π_3^*	−1.4444996	0.0000000	0.0000000
	π_2-π_4^*	0.0000000	−1.4439515	0.0000000
trans-1,3-butadiene	π_1-π_2^*	−1.5032934	−1.5671740	0.0000000

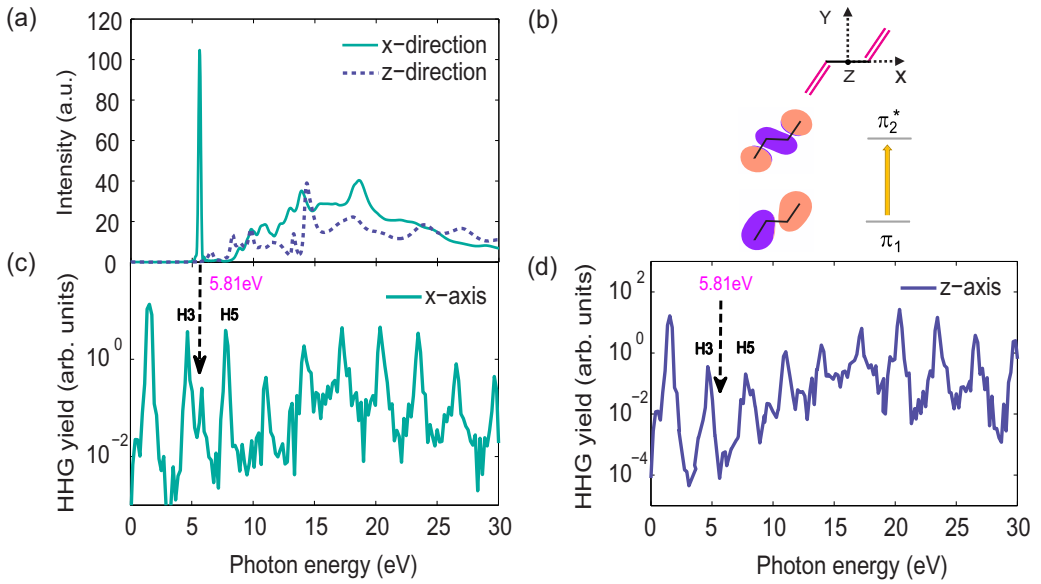

FIG. 2. (a) The optical absorption spectra of the *trans*-1,3-butadiene for the x and z directions. (b) The schematic illustration of the π-π^* transition between HOMO (π_1) and LUMO (π_2^*) of the *trans*-1,3-butadiene molecule in the optical absorption response. The geometrical configuration of the *trans*-1,3-butadiene and the coordinate system are presented at the top. (c) and (d) The high-harmonic spectra of the *trans*-1,3-butadiene driven by laser pulses polarized in the x axis and z axis, respectively. The wavelength of the laser pulse is 800 nm and the laser intensity is 8×10^{13} W/cm^2.

electrons may be pumped up to LUMOs and then jump back to HOMOs, accompanied by an emission of a photon. Figure 1(d) presents the harmonic spectrum of the benzene driven by a laser pulse polarized in the z axis. Herein, the noninteger order radiation peak does not appear. This result is consistent with the fact that the π-π^* transition in the z direction is forbidden.

The *trans*-1,3-butadiene is also adopted to probe the π-π^* transition in the harmonic spectrum. The geometrical configuration of the *trans*-1,3-butadiene molecule and the coordinate system are presented at the top of Fig. 2(b). The optical absorption spectra of the *trans*-1,3-butadiene for the x and z directions are shown in Fig. 2(a). The kick momentum κ and evolution time duration T are the same as those chosen for the benzene. One can see a sharp peak at 5.81 eV in the absorption spectrum for the x direction. As illustrated in Fig. 2(b), the absorption is also caused by the π-π^* transition between the HOMO (π_1) and LUMO (π_2^*) of the *trans*-1,3-butadiene. The position of the absorption peak is in agreement with that observed experimentally and calculated theoretically, where the excitation energy ΔE is around 5.69 eV ($\lambda_{\max} \approx 217.9$ nm) [19,57–59]. The π-π^* transition peak is not found in the absorption spectrum for the z direction shown in Fig. 2(a). This indicates that the transition in the vertical direction is forbidden, which is confirmed by the zero value of the z component of $\mathbf{d}_{\pi\text{-}\pi^*}$ as shown in Table I. Figures 2(c) and 2(d) present the harmonic spectra of the *trans*-1,3-butadiene molecule driven by the laser pulses polarized in the x axis and z axis, respectively. The wavelength and intensity of the laser pulse are the same as those chosen for the benzene molecule. A prominent noninteger order peak is found in the harmonic spectrum between the third harmonic and the fifth harmonic in Fig. 2(c). The photon energy of the radiation peak corresponds to the π-π^* excitation energy 5.81 eV as shown in Fig. 2(a). This correspondence also implies that the radiation may result from the transition from the LUMO (π_2^*) to HOMO (π_1). The absence of the noninteger order peak in Fig. 2(d) is consistent with the fact that the corresponding π-π^* transition is forbidden in the z direction as shown in Table I.

The mechanism of the noninteger order radiations for the benzene and *trans*-1,3-butadiene are further examined by varying the laser wavelengths from 740 to 920 nm. Figures 3(a)–3(d) and 3(e)-3(h) show the harmonic spectra at the energy region ranging from 3 to 13 eV for the benzene and *trans*-1,3-butadiene, respectively. Herein, the laser intensity is 8×10^{13} W/cm^2 and the laser pulse is polarized along the x axis. The linearity coordinates are adopted for much clearer observations of the radiation peaks. The pink dashed vertical lines indicate the excitation energies ΔE of π-π^* transitions. One can see that the noninteger order radiation peaks appear in all the figures except Fig. 3(d) (this will be explained later). It indicates that this noninteger order radiation is a general phenomenon. Moreover, the peaks always locate at the positions corresponding to the π-π^* excitation energies ΔE. This confirms that the noninteger order radiations are due to the π-π^* transitions in conjugated compounds, being independent of the driving laser wavelength. The gray dashed diagonal lines indicate the fifth harmonic, which gradually approaches the noninteger order radiation peak with increasing the laser wavelength. In addition, the harmonic efficiencies generally decrease with increasing the laser wavelength. This is due to the wavelength scaling law [60] of HHG. It is worth noting that a prominent enhancement occurs for the benzene with the wavelength of 920 nm as shown in Fig. 3(d). This is caused by a resonance effect [61–64] due to the overlap of the π-π^* radiation peak and the fifth harmonic peak, where ΔE, right, equals five times the photon energy of the driving laser. Compared with the resonance enhancement of the HHG from previous observations in atoms or plasma

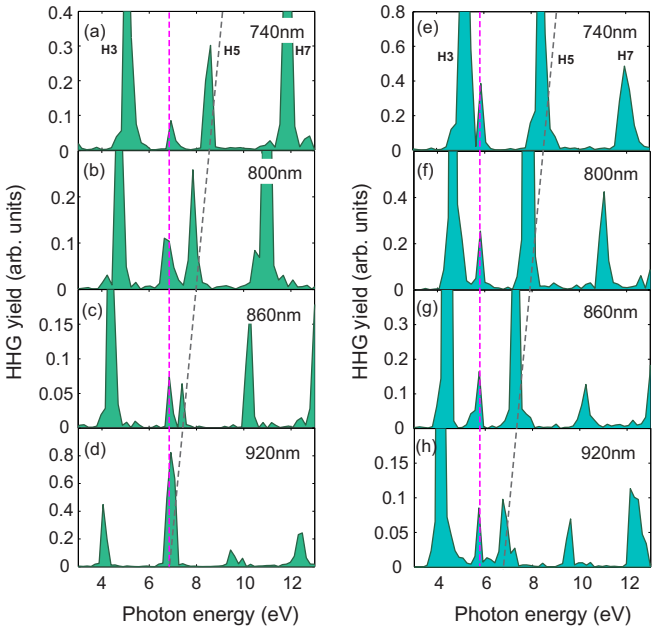

FIG. 3. High-harmonic spectra of the (a)–(d) benzene and (e)–(h) *trans*-1,3-butadiene by varying the laser wavelength ranging from 740 to 920 nm. The laser pulse is polarized along the x axis, and the laser intensity is 8×10^{13} W/cm^2. The pink dashed vertical lines indicate the excitation energies of π-π^* transitions. The gray dashed diagonal lines indicate the fifth harmonic.

plumes (such as GaAs, InSb, etc.) [65], this signal in large organic conjugated molecules originates from the transition between the characteristic π and π^* orbitals and contains significant information of the molecular dynamics.

In order to further confirm the mechanism of noninteger order radiations, we study the intensity variations of integer and noninteger order radiations by varying the polarization direction of the laser pulse. The polarization direction of the laser pulse rotates in the x-z plane from the x axis to the z axis, and is described by the elevation angle ϕ as shown in Figs. 4(a) and 4(b). The elevation angle ϕ is defined as the included angle of x axis and the polarization direction of the laser pulse.

Figure 4 shows the normalized radiation intensities of the components parallel to the polarization direction of the driving laser field. The results for the benzene are shown in Fig. 4(c) and those for *trans*-1,3-butadiene are shown in Fig. 4(d). The wavelength is 800 nm and the laser intensity is 8×10^{13} W/cm^2. The normalized intensities of the 3rd, 5th, and 11th harmonics are denoted as H3, H5, and H11, respectively. One can see that the normalized intensities of integer order harmonics decrease firstly, reach their minimum at about 50°, and increase with further increasing the elevation angle ϕ. The variations of intensities of the parallel component form U-shaped curves. By contrast, for noninteger order radiations, the normalized intensities of the parallel components, denoted as $H_{\pi\text{-}\pi^*}$, decrease monotonously with increasing ϕ. The different tendencies indicate that integer order harmonics and noninteger order radiations result from different physical mechanisms. In order to validate that the noninteger order radiations are closely related to π-π^* radiations, the normalized dipole transition probability $|\mathbf{d}^{\phi}_{\pi\text{-}\pi^*}|^2$ are calculated, where $\mathbf{d}^{\phi}_{\pi\text{-}\pi^*}$ is the transition dipole component parallel to the driving laser. The normalized $|\mathbf{d}^{\phi}_{\pi\text{-}\pi^*}|^2$ curves are shown in Figs. 4(c) and 4(d). One can see that the $H_{\pi\text{-}\pi^*}$ curves are in good agreement with the $|\mathbf{d}^{\phi}_{\pi\text{-}\pi^*}|^2$ curves. Our results further verify that the noninteger order radiations for conjugated compounds are caused by the π-π^* transition mechanism, i.e., the radiations stem from the π-π^* transitions from the LUMOs to HOMOs. It is worth noting that the

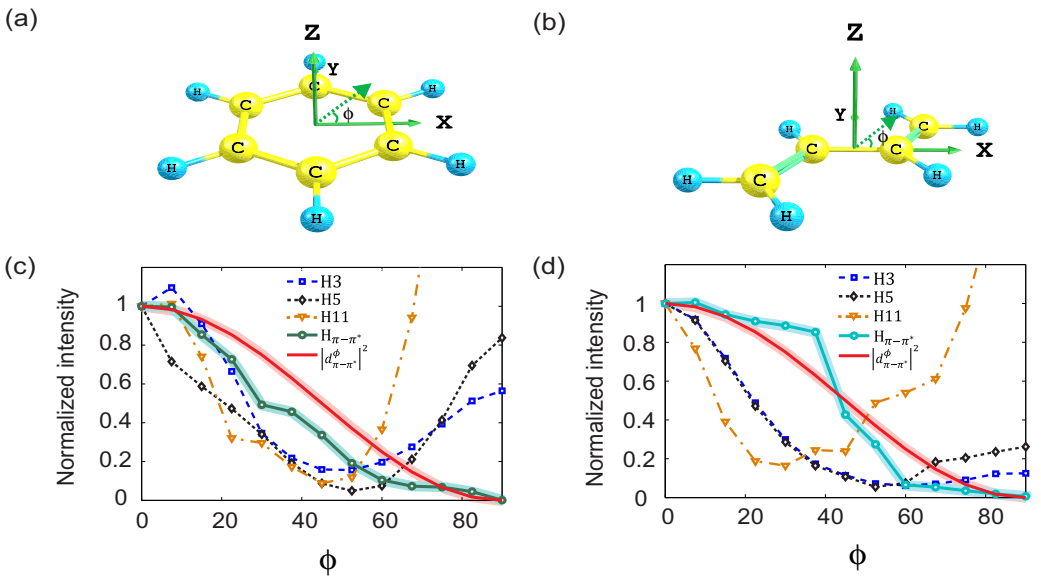

FIG. 4. (a) and (b) The schematic illustrations of geometrical configuration and elevation angle ϕ for the benzene and *trans*-1,3-butadiene, respectively. (c) and (d) The normalized intensities of the parallel component for the H3, H5, H11, and the π-π^* transition radiation for the benzene and *trans*-1,3-butadiene, respectively. $|\mathbf{d}^{\phi}_{\pi\text{-}\pi^*}|^2$ presents the modulus square of the transition dipole component parallel to the driving laser. ϕ varies from 0° to 90°. The wavelength of the laser pulse is 800 nm and the laser intensity is 8×10^{13} W/cm^2.

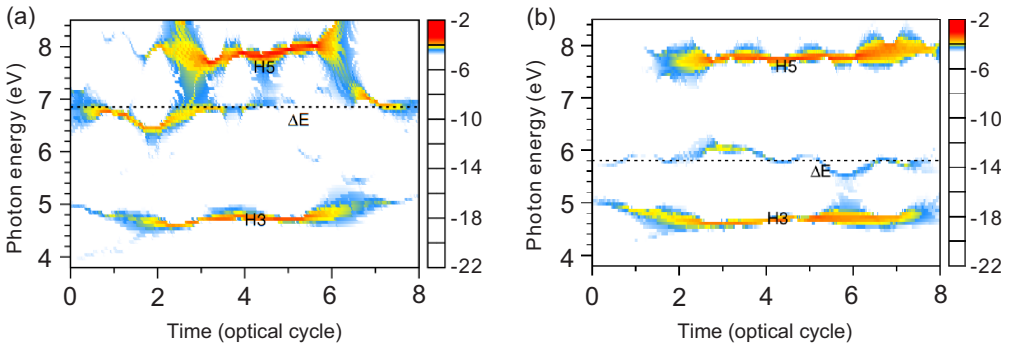

FIG. 5. The time-frequency spectra calculated by SST for (a) benzene and (b) *trans*-1,3-butadiene. The laser pulse is polarized along the x axis. The wavelength of the laser pulse is 800 nm and the laser intensity is 8×10^{13} W/cm^2. The dashed horizontal lines indicate the excitation energies ΔE of π-π^* transitions.

radiations can be observed in high-harmonic spectra only when the corresponding transition probabilities are large enough for various atoms and molecules. In the conjugated molecules, the π-π^* radiations can more easily show up in the harmonics spectra because the transitions between the conjugated π-type HOMO(s) and LUMO(s) are typically very strong. In this work, the π-π^* radiations from aligned molecules are discussed. Since the π-π^* radiations can take place in all directions except for the directions along the $\pm z$ axis when the polarization directions of the laser pulses vary, the π-π^* transition signal will survive an orientational averaging if a randomly aligned molecular sample is considered.

The duration of the bound-bound emission is also a significant feature to reveal the underlying mechanism. For example, distinct time decays of radiations are found in the FID process [39] and resonance-enhanced HHG [62]. In order to shed light on the π-π^* radiation process unambiguously, we study the emission times by performing the time-frequency (TF) analysis. The TF spectra are calculated using the synchrosqueezing transform (SST) [66]. Compared with traditional TF techniques (such as Gabor transform, Morlet transform, etc.), the SST can resolve the intrinsic blurring in the TF spectrum below the ionization threshold and produce a clear spectrum [67]. Figures 5(a) and 5(b) show the TF spectra for benzene and *trans*-1,3-butadiene with the same laser parameters adopted in Fig. 1(c), respectively. One can clearly see three radiation signals in the TF spectra, i.e., H3, π-π^* radiation (indicated by ΔE), and H5. For the benzene, one can see a competition between the H5 radiation and π-π^* radiation since the ΔE is close to the photon energy of H5 as shown in Fig. 5(a). Specifically, the π-π^* radiation is dominant in the rising part of the pulse (zero to two optical cycles) with low laser intensity firstly. Then H5 radiation becomes dominant in the plateau of the pulse (two to six optical cycles) with high laser intensity, and the π-π^* radiation becomes weak. Finally, the π-π^* radiation dominates again in the falling part of the pulse (six to eight optical cycles) when the laser intensity decreases. For the *trans*-1,3-butadiene, ΔE is close to the photon energy of H3 as shown in Fig. 5(b). The H3 signal is always dominant, and the π-π^* radiation is always comparatively weak. Concerning the emission times of the π-π^* radiation for both benzene and *trans*-1,3-butadiene, there is no obvious time delay. This is because lifetimes of the excited states (LUMOs) in the π-π^* radiation processes are shorter in comparison to the typical FID and resonance-enhanced HHG processes.

IV. CONCLUSION

In summary, we demonstrate that the HHS provides a direct approach to probe the π-π^* transition in conjugated compounds. More specifically, a noninteger order radiation whose energy accurately matches the π-π^* excitation energy is observed in the harmonic spectrum. Our study further confirms that the radiation originates from the π-π^* transition mechanism by scanning laser wavelengths and studying the elevation angle dependence of the integer and noninteger order signals. Our HHS approach offers a useful tool to study the π-π^* transitions of conjugated compounds. Compared with a conventional optical absorption method with SR source, our scheme, performed with a single beam of femtosecond laser pulse, considerably simplifies the experimental setup. This work opens a promising route to probe excited-state dynamics and photoexcitation processes in their natural time scale.

ACKNOWLEDGMENTS

The authors thank Professor Ruifeng Lu for very helpful discussions. This work was supported by the National Natural Science Foundation of China under Grants No. 11422435, No. 11404123, No. 11234004, and No. 11627809. Numerical simulations presented in this paper were carried out using the High Performance Computing Center experimental test bed in SCTS/CGCL.

[1] P. Tavan and K. Schulten, Phys. Rev. B **36**, 4337 (1987).

[2] S. Takeuchi, S. Ruhman, T. Tsuneda, M. Chiba, T. Taketsugu, and T. Tahara, Science **322**, 1073 (2008).

[3] H. C. Longuet-Higgins and E. W. Abrahamson, J. Am. Chem. Soc. **87**, 2045 (1965).

[4] R. B. Woodward and R. Hoffmann, Angew. Chem., Int. Ed. **8**, 781 (1969).

[5] M. C. Yoon, Y. S. Choi, and S. K. Kim, Chem. Phys. Lett. **300**, 207 (1999).

[6] P. Schwille, S. Kummer, A. A. Heikal, W. E. Moerner, and W. W. Webb, Proc. Natl. Acad. Sci. USA **97**, 151 (2000).

[7] M. A. L. Marques, X. López, D. Varsano, A. Castro, and A. Rubio, Phys. Rev. Lett. **90**, 258101 (2003); C. Camilloni, D. Provasi, G. Tiana, and R. A. Broglia, J. Phys. Chem. B **111**, 10807 (2007); R. A. G. Cinelli, V. Tozzini, V. Pellegrini, F. Beltram, G. Cerullo, M. Zavelani-Rossi, S. De Silvestri, M. Tyagi, and M. Giacca, Phys. Rev. Lett. **86**, 3439 (2001).

[8] D. Varsano, A. Garbesi, and R. D. Felice, J. Phys. Chem. B **111**, 14012 (2007).

[9] Y. Morisawa, M. Yasunaga, H. Sato, R. Fukuda, M. Ehara, and Y. Ozaki, J. Phys. Chem. B **118**, 11855 (2014).

[10] K. Schulten, U. Dinur, and B. Honig, J. Chem. Phys. **73**, 3927 (1980).

[11] H. A. Kurtz and K. D. Jordan, J. Chem. Phys. **72**, 493 (1980).

[12] T. Hashimoto, H. Nakano, and K. Hirao, J. Chem. Phys. **104**, 6244 (1996).

[13] P. Strodel and P. Tavan, J. Chem. Phys. **117**, 4677 (2002).

[14] K. L. D'Amico, C. Manos, and R. L. Christensen, J. Am. Chem. Soc. **102**, 1777 (1980).

[15] J. P. Doering and R. McDiarmid, J. Chem. Phys. **73**, 3617 (1980).

[16] K. Yabana and G. F. Bertsch, Int. J. Quantum. Chem. **75**, 55 (1999).

[17] S. Grimm, C. Nonnenberg, and I. Frank, J. Chem. Phys. **119**, 11574 (2003).

[18] X. Lopez and M. A. L. Marques, Lect. Notes Phys. **706**, 323 (2006).

[19] R. R. Chadwick, M. Z. Zgierski, and B. S. Hudson, J. Chem. Phys. **95**, 7204 (1991).

[20] E. E. Koch and A. Otto, Chem. Phys. Lett. **12**, 476 (1972).

[21] A. Hiraya and K. Shobatake, J. Chem. Phys. **94**, 7700 (1991).

[22] R. W. Schoenlein, S. Chattopadhyay, H. H. W. Chong, T. E. Glover, P. A. Heimann, C. V. Shank, A. A. Zholents, and M. S. Zolotorev, Science **287**, 2237 (2000).

[23] F. Krausz and M. Ivanov, Rev. Mod. Phys. **81**, 163 (2009).

[24] P. B. Corkum and F. Krausz, Nat. Phys. **3**, 381 (2007).

[25] L. Fechner, N. Camus, J. Ullrich, T. Pfeifer, and R. Moshammer, Phys. Rev. Lett. **112**, 213001 (2014); L. Yue and L. B. Madsen, Phys. Rev. A **90**, 063408 (2014); M. He, Y. Li, Y. Zhou, M. Li, and P. Lu, *ibid.* **93**, 033406 (2016); A. H. Tong, Y. M. Zhou, and P. X. Lu, Opt. Quantum Electron. **49**, 77 (2017); Sci. Sin. Phys., Mech. Astron. **47**, 033005 (2017).

[26] P. B. Corkum, Phys. Rev. Lett. **71**, 1994 (1993); M. Lewenstein, P. Balcou, M. Y. Ivanov, A. L'Huillier, and P. B. Corkum, Phys. Rev. A **49**, 2117 (1994); L. He, P. Lan, Q. Zhang, C. Zhai, F. Wang, W. Shi, and P. Lu, *ibid.* **92**, 043403 (2015); L. Li, Z. Wang, F. Li, and H. Long, Opt. Quantum Electron. **49**, 73 (2017); X. Zhang, X. Zhu, X. Liu, D. Wang, Q. Zhang, P. Lan, and P. Lu, Opt. Lett. **42**, 1027 (2017).

[27] J. Itatani, J. Levesque, D. Zeidler, H. Niikura, H. Pépin, J. C. Kieffer, P. B. Corkum, and D. M. Villeneuve, Nature (London) **432**, 867 (2004).

[28] S. Haessler, J. Caillat, W. Boutu, C. Giovanetti-Teixeira, T. Ruchon, T. Auguste, Z. Diveki, P. Breger, A. Maquet, B. Carré, R. Taïeb, and P. Salières, Nat. Phys. **6**, 200 (2010).

[29] C. Vozzi, M. Negro, F. Calegari, G. Sansone, M. Nisoli, S. D. Silvestri, and S. Stagira, Nat. Phys. **7**, 822 (2011).

[30] X. Zhu, M. Qin, Q. Zhang, Y. Li, Z. Xu, and P. Lu, Opt. Express **21**, 5255 (2013); M. Qin and X. Zhu, Opt. Laser Technol. **87**, 79 (2017); C. Zhai, L. He, P. Lan, X. Zhu, Y. Li, F. Wang, W. Shi, Q. Zhang, and P. Lu, Sci. Rep. **6**, 23236 (2016).

[31] R. Cireasa, A. E. Boguslavskiy, B. Pons, M. C. H. Wong, D. Descamps, S. Petit, H. Ruf, N. Thiré, A. Ferré, J. Suarez, J. Higuet, B. E. Schmidt, A. F. Alharbi, F. Légaré, V. Blanchet, B. Fabre, S. Patchkovskii, O. Smirnova, Y. Mairesse, and V. R. Bhardwaj, Nat. Phys. **11**, 654 (2015).

[32] O. Smirnova, Y. Mairesse, and S. Patchkovskii, J. Phys. B: At., Mol. Opt. Phys. **48**, 234005 (2015).

[33] X. Zhu, X. Liu, P. Lan, D. Wang, Q. Zhang, W. Li, and P. Lu, Opt. Express **24**, 24824 (2016).

[34] O. Smirnova, Y. Mairesse, S. Patchkovskii, N. Dudovich, D. Villeneuve, P. Corkum, and M. Y. Ivanov, Nature (London) **460**, 972 (2009).

[35] P. M. Kraus, B. Mignolet, D. Baykusheva, A. Rupenyan, L. Horný, E. F. Penka, G. Grassi, O. I. Tolstikhin, J. Schneider, F. Jensen, L. B. Madsen, A. D. Bandrauk, F. Remacle, and H. J. Wörner, Science **350**, 790 (2015).

[36] H. J. Wörner, J. B. Bertrand, D. V. Kartashov, P. B. Corkum, and D. M. Villeneuve, Nature (London) **466**, 604 (2010).

[37] X. Zhou, P. Ranitovic, C. W. Hogle, J. H. D. Eland, H. C. Kapteyn, and M. M. Murnane, Nat. Phys. **8**, 232 (2012).

[38] W. Li, X. Zhou, R. Lock, S. Patchkovskii, A. Stolow, H. C. Kapteyn, and M. M. Murnane, Science **322**, 1207 (2008).

[39] S. Beaulieu, S. Camp, D. Descamps, A. Comby, V. Wanie, S. Petit, F. Légaré, K. J. Schafer, M. B. Gaarde, F. Catoire, and Y. Mairesse, Phys. Rev. Lett. **117**, 203001 (2016).

[40] X. B. Bian and A. D. Bandrauk, Phys. Rev. Lett. **105**, 093903 (2010).

[41] X. B. Bian and A. D. Bandrauk, Appl. Sci. **3**, 267 (2013).

[42] S. Camp, K. J. Schafer, and M. B. Gaarde, Phys. Rev. A **92**, 013404 (2015).

[43] A. R. Beck, B. Bernhardt, E. R. Warrick, M. Wu, S. Chen, M. B. Gaarde, K. J. Schafer, D. M. Neumark, and S. R. Leone, New J. Phys. **16**, 113016 (2014).

[44] E. Runge and E. K. U. Gross, Phys. Rev. Lett. **52**, 997 (1984).

[45] H. Yun, K. M. Lee, J. H. Sung, K. T. Kim, H. T. Kim, and C. H. Nam, Phys. Rev. Lett. **114**, 153901 (2015).

[46] X. Chu and G. C. Groenenboom, Phys. Rev. A **93**, 013422 (2016).

[47] X. L. Lozano, C. Mottet, and H. C. Weissker, J. Phys. Chem. C **117**, 3062 (2013).

[48] H. C. Weissker, O. Lopez-Acevedo, R. L. Whetten, and X. López-Lozano, J. Phys. Chem. C **119**, 11250 (2015).

[49] R. W. Burgess and V. J. Keast, J. Phys. Chem. C **118**, 3194 (2014).

[50] X. Liu, X. Zhu, L. Li, Y. Li, Q. Zhang, P. Lan, and P. Lu, Phys. Rev. A **94**, 033410 (2016).

[51] J. P. Perdew, K. Burke, and M. Ernzerhof, Phys. Rev. Lett. **77**, 3865 (1996).

[52] C. Hartwigsen, S. Goedecker, and J. Hutter, Phys. Rev. B **58**, 3641 (1998).

[53] A. Castro, M. A. L. Marques, and A. Rubio, J. Chem. Phys. **121**, 3425 (2004).

[54] K. Yabana and G. F. Bertsch, Phys. Rev. B **54**, 4484 (1996); G. Malloci, G. Cappellini, G. Mulas, and G. Satta, *ibid.* **70**, 205429 (2004); X. Lopez, M. A. L. Marques, A. Castro, and A. Rubio, J. Am. Chem. Soc. **127**, 12329 (2005); M. J. T. Oliveira, B. Mignolet, T. Kus, T. A. Papadopoulos, F. Remacle, and M. J. Verstraete, J. Chem. Theory Comput. **11**, 2221 (2015).

[55] M. A. L. Marques, A. Castro, G. F. Bertsch, and A. Rubio, Comput. Phys. Commun. **151**, 60 (2003); A. Castro, H. Appel, M. Oliveira, C. A. Rozzi, X. Andrade, F. Lorenzen, M. A. L. Marques, E. K. U. Gross, and A. Rubio, Phys. Status Solidi B **243**, 2465 (2006); X. Andrade and A. Aspuru-Guzik, J. Chem. Theory Comput. **9**, 4360 (2013).

[56] M. J. S. Dewar and W. Thiel, J. Am. Chem. Soc. **99**, 4907 (1977).

[57] O. A. Mosher, W. M. Flicker, and A. Kuppermann, J. Chem. Phys. **59**, 6502 (1973).

[58] G. Müller, K. D. Gneuss, H. P. Kriemler, A. I. Scott, and A. I. Irwin, J. Am. Chem. Soc. **101**, 3657 (1979).

[59] R. P. Krawczyk, K. Malsch, G. Hohlneicher, R. C. Gillen, and W. Domcke, Chem. Phys. Lett. **320**, 535 (2000).

[60] K. Schiessl, K. L. Ishikawa, E. Persson, and J. Burgdörfer, Phys. Rev. Lett. **99**, 253903 (2007).

[61] S. Haessler, L. B. E. Bom, O. Gobert, J. F. Hergott, F. Lepetit, M. Perdrix, B. Carré, T. Ozaki, and P. Salières, J. Phys. B: At., Mol. Opt. Phys. **45**, 074012 (2012).

[62] R. A. Ganeev, Z. Wang, P. Lan, P. Lu, M. Suzuki, and H. Kuroda, Phys. Rev. A **93**, 043848 (2016).

[63] R. A. Ganeev, M. Suzuki, M. Baba, and H. Kuroda, Opt. Lett. **31**, 1699 (2006).

[64] M. Li, P. Zhang, S. Luo, Y. Zhou, Q. Zhang, P. Lan, and P. Lu, Phys. Rev. A **92**, 063404 (2015); X. Zhu, P. Lan, K. Liu, Y. Li, X. Liu, Q. Zhang, I. Barth, and P. Lu, Opt. Express **24**, 4196 (2016).

[65] R. A. Ganeev, J. Phys. B: At., Mol. Opt. Phys. **40**, R213 (2007).

[66] Y. L. Sheu, L. Y. Hsu, H. T. Wu, P. C. Li, and S. I. Chu, AIP Adv. **4**, 117138 (2014).

[67] P. C. Li, Y. L. Sheu, C. Laughlin, and S. I. Chu, Nat. Commun. **6**, 7178 (2015).